

PROCEEDINGS OF SPIE

SPIDigitalLibrary.org/conference-proceedings-of-spie

Advanced metal processing enabled by fiber lasers with tunable beam properties

Kliner, Dahv, Farrow, R., Lugo, J., O'Dea, B., Hawke, R., et al.

Dahv A. Kliner, R. L. Farrow, J. Lugo, B. O'Dea, R. Hawke, B. Victor, K. Gross, A. Hodges, A. Brown, J. Pruyn, R. Stephens, R. Stephens, B. Foley, K. Almonte, B. Kehoe, M. Hamilton, M. Reynolds, C. Luetjen, T. Lowder, S. Karlsen, D. Balsley, M. Antoina, T. Kokki, D. Swenson, C. Archer, R. Martinsen, M. Hepp, "Advanced metal processing enabled by fiber lasers with tunable beam properties," Proc. SPIE 11981, Fiber Lasers XIX: Technology and Systems, 119810C (4 March 2022); doi: 10.1117/12.2614728

SPIE.

Event: SPIE LASE, 2022, San Francisco, California, United States

Advanced metal processing enabled by fiber lasers with tunable beam properties

D.A.V. Kliner*, R.L. Farrow, J. Lugo, B. O’Dea, R. Hawke, B. Victor, K. Gross, A. Hodges, A. Brown, J. Pruyn, R. Stephens, B. Foley, K. Almonte, B. Kehoe, M. Hamilton, M. Reynolds, C. Luetjen, T. Lowder, S. Karlsen, D. Balsley, M. Antoina, T. Kokki, D. Swenson, C. Archer, R. Martinsen, and M. Hepp
nLIGHT, 5408 NE 88th Street, Building E, Vancouver, WA 98665 USA

ABSTRACT

Lasers are essential tools for a wide variety of materials processing applications. The speed, quality, and process window are determined in part by the laser beam properties, including size, shape, and divergence. Most laser sources have fixed beam characteristics, resulting in processing and material limitations and nonoptimized performance. nLIGHT has developed a fiber-laser product line that provides rapid tunability of the beam characteristics directly from the delivery fiber using a novel, all-fiber mechanism. The broad range of beam sizes and shapes and real-time programmability allow adjustments on-the-fly and optimization of each process step using a single laser source, enabling development of versatile tools that provide optimum performance for a range of processing needs. We describe the underlying technology, performance, and beam characteristics and show results for the largest industrial laser applications, including metal cutting, welding, and additive manufacturing.

Keywords: Fiber laser, variable beam, beam shape, materials processing, laser cutting, laser welding, additive manufacturing, laser powder-bed fusion (L-PBF)

1. INTRODUCTION

Lasers have become indispensable tools for manufacturing, with 2021 laser revenue estimated to be >\$6 billion for materials-processing and lithography applications.¹ Laser-based processing has steadily expanded its share of the ~\$100 billion annual machine-tool market, driven by significant advances in laser performance and practicality in the key areas of average- and peak-power capability, wavelength coverage, temporal versatility (pulse duration and frequency, sophisticated waveforms), electrical efficiency, power stability and tunability, long-term reliability, maintenance requirements, and upfront and operating costs.² Fiber lasers have been particularly important in enabling many of these advances³ and now dominate the highest-volume industrial and microfabrication applications. In addition to their high efficiency and reliability, fiber lasers naturally enable fiber delivery to the process head, minimizing the burden of free-space optics within both the laser and the machine tool.

In contrast to other important specifications, laser beam spatial characteristics remain relatively unoptimized and inflexible. The beam spatial properties influence heat deposition, temperature gradients, and the thermal profile in the workpiece, which are key determinants of processing speed and material quality and thus of tool productivity and part cost. Some applications require diffraction-limited beam quality (a near-Gaussian spatial profile with $M^2 \approx 1$), whereas others require lower beam quality and distinct near-field spatial profiles, far-field divergence profiles, and propagation characteristics. Useful spatial profiles include flat-tops and ring beams, saddle beams (i.e., annular beams with some intensity in the center), and beams with a surrounding halo or pedestal, all with various sizes. Within a particular application or tool, different beam properties are typically required to optimize different jobs (different materials, thicknesses, part dimensions, etc.). Even within a given job or part, different beam properties may be required to optimize different process steps (various feature sizes or geometries, piercing vs. cutting, etc.).

Because the beam characteristics of most lasers are fixed, tool integrators and end users must either add downstream components that provide beam tunability or accept limited tool capabilities and versatility. The former approach adds complexity and cost and/or degrades performance and reliability of the tool. The latter approach results in nonoptimal processing performance, a limited job mix, and/or the need to purchase multiple tools. To address this long-standing problem, nLIGHT developed a novel, all-fiber technology (Corona™) that provides rapidly tunable beam characteristics

*dahv.kliner@nlight.net; phone +1-925-719-7070; nlight.net

directly from the laser output fiber (feeding fiber) at multi-kW power levels.^{4,5} Corona technology offers a palette of optimized beam sizes and shapes, with a wide range of specifications available with different fiber designs. We have released Corona-based multimode fiber lasers (CFX™) up to 15 kW and single-mode fiber lasers (AFX™) up to 1.2 kW. These products have shown groundbreaking performance in the largest established and emerging industrial metal-processing applications of cutting, welding, and additive manufacturing (AM). Leading tool integrators have introduced a new generation of versatile, high-performance tools enabled by CFX and AFX fiber lasers, and these tools have been installed in production facilities worldwide.

Section 2 summarizes previous approaches to generate tunable beams and then describes Corona all-fiber technology. Sections 3, 4, and 5 describe the application of CFX and AFX fiber lasers to metal cutting, welding, and additive manufacturing, respectively; these sections include descriptions of the tunable beam properties that have been optimized for these important applications. Finally, Section 6 presents conclusions. Previous publications describe the technical underpinnings of Corona fiber lasers, as well as the first CFX products and their use in metal cutting and welding; rather than repeat this information, Sections 2 – 5 provide brief summaries and reference the relevant publications.

2. TECHNOLOGIES FOR BEAM TUNABILITY

2.1 Legacy approaches

Most lasers provide fixed beam characteristics, and the beam can be transformed to a different format by refractive, reflective, or diffractive optical systems. Approaches that provide some level of beam tunability include process heads with changeable optics, zoom lenses, switchable or tunable diffractive optical elements, deformable mirrors, beam combiners, and fiber couplers and switches with motorized optics. These free-space optical approaches have demonstrated the materials-processing benefits of being able to change the beam properties, but they entail several drawbacks:

- Sensitivity to contamination, misalignment, and environmental conditions (temperature, shock, vibration).
- Increased system cost and complexity.
- Optical loss.
- Thermal lensing in high-power applications, causing power-dependent changes in beam quality and focus position (these changes can also be time dependent as optics degrade, e.g., from contamination).
- In the case of manually changeable optics, loss of productivity, risk of contamination and damage, and incompatibility with automated production.
- In the case of zoom lenses, increased size and weight of the process head.

Fiber-based beam combination has been used to provide specific beam shapes with some tunability. In these systems, the feeding fiber typically consists of a central core and a surrounding annular core, with different lasers launched into these two cores via a fused-fiber combiner. This approach has the advantage of eliminating free-space optics, at the cost of other drawbacks:

- The division of power between the regions is “hardwired” when the laser is manufactured and cannot be changed to accommodate different processes or materials, limiting the versatility of the tool.
- The full laser power is available in only one beam shape. Changing the beam shape entails turning down the power in one of the guiding regions. For applications that require beam tuning, the end user is thus forced to purchase extra laser power, incurring significant cost.
- The available beam shapes are limited. This approach provides one annular beam size and shape from the feeding fiber. Obtaining different annular beams from a given laser would require addition of a zoom lens or other free-space optics, undermining the primary benefit of the beam-combination technology.

Because available options providing beam tunability entail significant compromises in tool complexity, cost, performance, versatility, and/or reliability, most laser-based tools employ a fixed beam, resulting in nonoptimal performance and/or a limited job mix. Some shops purchase multiple tools optimized for different tasks to address their range of processing needs.

2.2 All-fiber beam tunability: nLIGHT Corona

We developed an all-fiber technology (Corona) to deliver a wide range of beam shapes and sizes directly from the laser feeding fiber. We have released several fiber laser products incorporating this technology spanning the power range of <500 W to 15 kW, with beam characteristics optimized for the largest industrial metal-processing applications. We had several design goals to maximize the performance, productivity, versatility, and reliability of machine tools incorporating Corona fiber lasers:

- All fiber – To eliminate the well-known performance and reliability problems associated with free-space optics (see Section 2.1).
- Compatibility with fixed-optic process heads – Ability to change the beam size without requiring a zoom lens.
- Integrated into the laser – No requirement for downstream optical components or special process fibers, which increase cost and introduce new failure modes.
- Full power available in all beam shapes – Minimize cost by allowing full utilization of the available laser power in all applications and process steps.
- Optimized power distributions – Materials-processing studies had shown the need for various beam sizes and shapes (Gaussian, flat-top, ring, pedestal, saddle) to maximize productivity and part quality.
- Fast switching on-the-fly – Enables optimization of each process step by real-time control of the beam properties with no need to blank the laser or interrupt the manufacturing process.

Our technical approach is described in Refs. 4 and 5. Briefly, the all-fiber Corona mechanism includes the following components:⁶

1. A feeding fiber that is segmented into multiple guiding regions. The beam shape is tuned by varying the partitioning of the laser power among these regions.
2. A length of fiber whose design enables the beam to be shifted radially via application of a perturbation. This shifting results in the desired tunable beam partitioning among the guiding regions of the feeding fiber.
3. A perturbation mechanism to shift the beam radially. Several effective perturbation mechanisms have been identified.⁶

The input beam to the Corona mechanism is delivered via fiber (from a fiber laser), and all fibers are spliced together, resulting in a continuous fiber path that maintains the performance and reliability benefits of traditional fiber lasers.

The number and dimensions of the guiding regions in the Corona feeding fiber can be optimized for different applications. Currently available Corona feeding fibers have a central core surrounded by either one or two annular guiding regions (“two-zone” and “three-zone” feeding fibers, respectively), and current products have the following designs:

- CFX – Both two-zone and three-zone feeding fibers are available. In all cases, the central core diameter is between 50 and 125 μm , and the outer annulus has an outside diameter (od) of 330 μm . In the three-zone products, the inner annulus has an od of either 175 μm or 215 μm . The beam-parameter-product (BPP) values span 2.0 to 18 mm-mrad.
- AFX – A two-zone feeding fiber is available. The central core provides a single-mode beam (mode-field diameter $\approx 14 \mu\text{m}$), and the surrounding annulus has an od of 40 μm . The M^2 values range from 1.2 to ~ 5 .

Corona feeding fibers are denoted “x/y” for two-zone and “x/y/z” for three-zone, where x, y, and z are the od values for the zones. For example, a feeding fiber with a 100 μm central core, a 215 μm inner annulus, and a 330 μm outer annulus is denoted “100/215/330.”

Figure 1 shows typical near-field spatial profiles and calculated beam diameters for three-zone (3 – 5 kW) and two-zone (6 – 15 kW) CFX fiber lasers used in metal cutting (beam profiles optimized for other applications are shown in Sections 3 – 5). We have found that supplying predefined beam shapes is preferable to continuous tuning of the beam for process optimization and stability. Industrial lasers are often deployed in electrically noisy environments, in which analog control signals can be unstable on a variety of timescales. By providing defined, digitally selectable (“programmable”) beam settings, the end user is ensured that their laser performance will be stable for years. The beam shapes, or “Index” settings, are numbered sequentially (0, 1, 2, ...), with larger values corresponding to more power partitioned into the ring(s) and thus larger calculated beam diameters. The number of Index settings and the power distribution among the guiding regions for each Index setting are software-settable and can be optimized based on the needs of the application or tool.

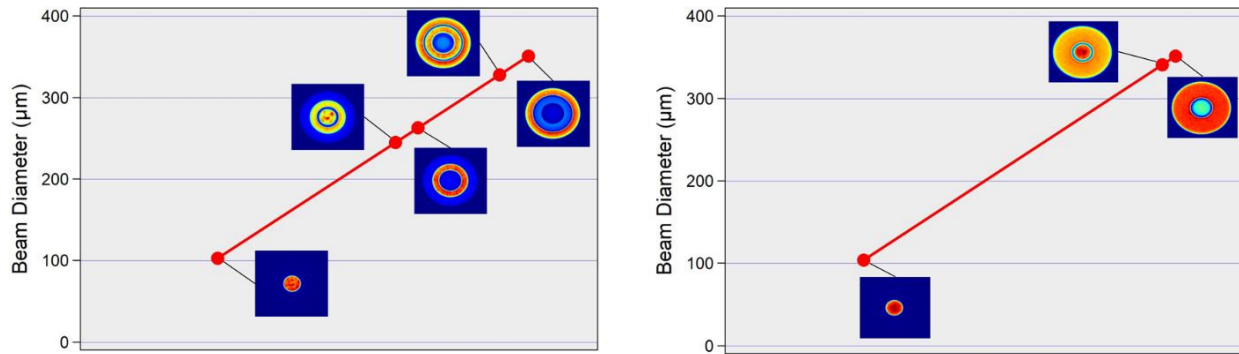


Figure 1. Typical beam settings for three-zone (100/215/330, left) and two-zone (100/330, right) CFX fiber lasers used in metal cutting. The images show near-field spatial profiles, and the corresponding second-moment ($D4\sigma$) beam diameters are given on the y-axes. Additional beam properties for CFX and AFX fiber lasers are presented in Sections 3 – 5.

It is evident from Fig. 1 that beams with significantly different shapes can have similar calculated beam diameters. A single metric (such as beam diameter, M^2 , BPP, etc.) does not provide a complete description of the beam nor uniquely determine its performance in a given material-processing application. We thus perform detailed characterization of both the near-field spatial profile and the far-field divergence distribution for all CFX and AFX fiber lasers to ensure consistent performance.

Because of Corona fiber lasers' unique approach to varying the beam properties, the full laser power is available for all Index settings. In some cases, the power or feeding-fiber length is limited to avoid deleterious nonlinear processes in the fiber (e.g., stimulated Raman scattering), as with conventional fiber lasers.

2.2.1. Switching speed

The switching time between Corona Index settings is typically <25 ms. Figure 2 shows near-field spatial profiles of a 5 kW, three-zone CFX fiber laser as the beam was switched from the smallest to the largest Index setting; the feeding-fiber design was the same as that shown on the left of Fig. 1 (100/215/330). The beam images were recorded with a CMOS camera with a 5 ms integration time. The smallest beam (Index 0) is a flat-top with a 100 μm od (0 ms image). The largest beam is a ring with a 330 μm od (images at times >30 ms). Transition of the beam through the guiding regions is evident in the images, with significant power in the intermediate guiding region (215 μm od) visible in the 10 ms image. The graph shows the calculated second-moment ($D4\sigma$) beam diameters. Note that the calculated ring-beam diameter is larger than the od, as expected for a second-moment calculation. The beam images and calculated diameters show that switching is complete by the third data point (31 ms), and the beam diameter then remains very stable with a standard deviation (σ) of 0.6 μm (0.2% of the measured diameter). The frame rate of the CMOS camera was insufficient to fully resolve the switching speed. Earlier measurements using a line-scan camera with a higher frame rate showed that switching is typically complete in <25 ms.⁴

2.2.2. Reproducibility and life tests

We investigated the reproducibility of the Corona beam settings by performing repeated measurements of the M^2 value after switching the Index setting. For example, we cycled an AFX laser 25 times among all seven Index settings and characterized the beam each time at each setting. For all Index settings, M^2 was repeatable to within $<2.9\%$ (3σ), which is comparable to the reproducibility of the M^2 tool, i.e., the extremely small variations in the AFX M^2 values were dominated by measurement uncertainty.

Accelerated life tests with >13 million beam changes in CFX and >20 million beam changes in AFX have shown excellent stability for the beam diameter and M^2 values. CFX results were presented in Ref. 4. AFX results are presented in Fig. 3, which shows M^2 measurements at each Index setting at the beginning of the life test, after 10 million Index changes, and after 21 million Index changes. The average deviation of the M^2 values from the mean is 2.2% (again dominated by measurement uncertainty).

These beam-switching and accelerated life tests show that Corona fiber lasers maintain the exceptional stability and reproducibility of conventional fiber lasers with fixed beam characteristics, and this performance pertains to all Index settings.

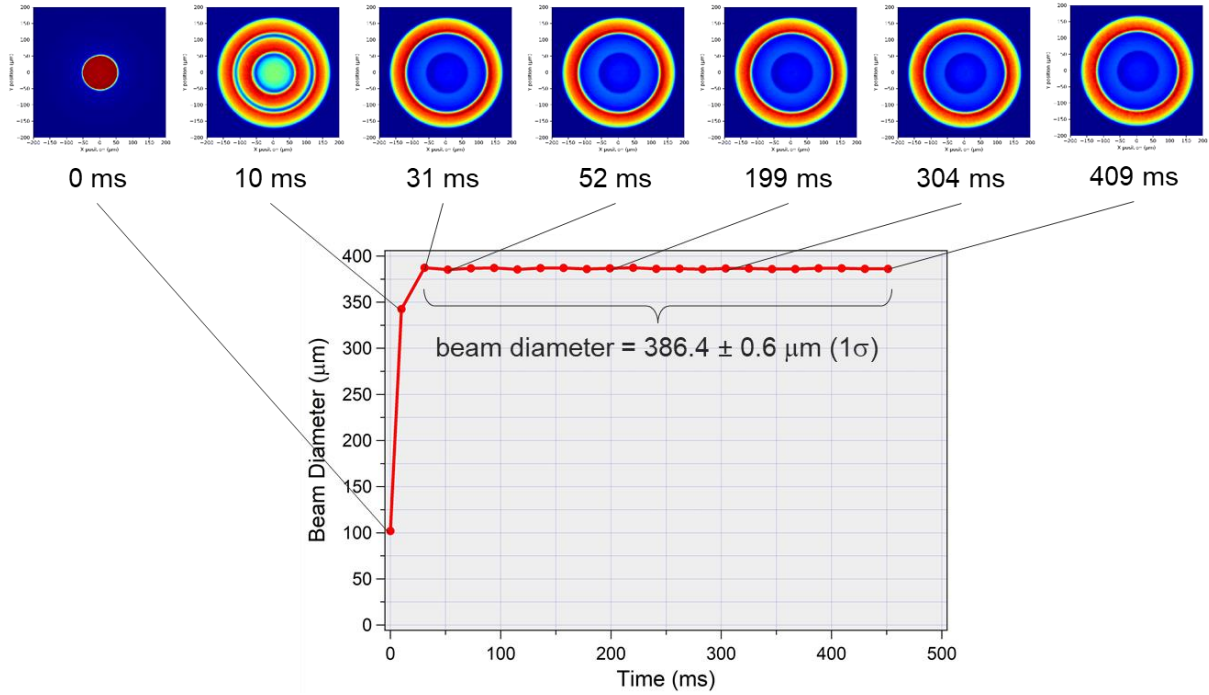


Figure 2. CMOS camera measurements of the near-field spatial profile (top images) and corresponding second-moment beam diameters while switching between the smallest and largest beam settings for a 5 kW CFX fiber laser with a three-zone (100/215/330) feeding fiber.

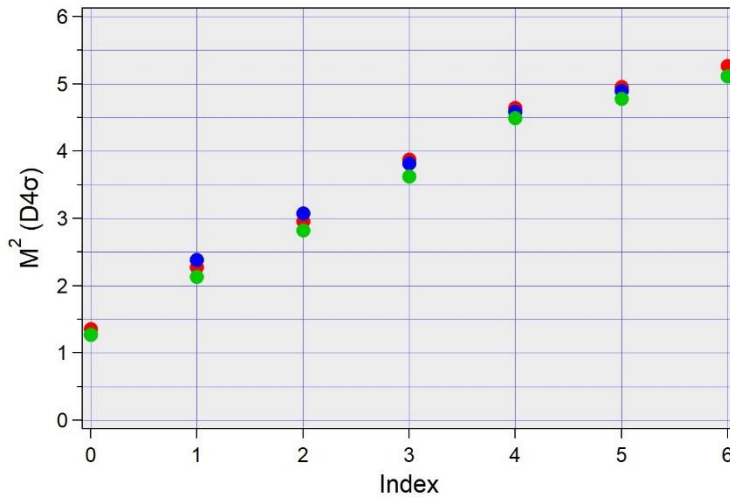


Figure 3. AFX accelerated life test. The red, blue, and green points show the M^2 values measured, respectively, at the beginning of the test, after 10 million Index changes, and after 21 million Index changes with the laser operating at full power.

2.2.3. Other CFX and AFX performance attributes

CFX and AFX fiber lasers retain all the standard benefits of other nLIGHT fiber lasers⁷, specifically:

- Hardware-based back-reflection protection that enables uninterrupted processing of highly reflective materials and finishes with no requirements to modify processing recipes or tool configurations.⁸
- Industry-leading power tunability (5 – 100%) and stability ($\sigma < 1\%$ over 8 hr). A unique feature of nLIGHT fiber lasers is that the power stability specification pertains over the full power range, i.e., the standard deviation of the power is $< 1\%$ of the set point for all power levels between 5% and 100% of full power.
- The fastest modulation rate (100 kHz) and rise and fall times ($< 5 \mu\text{s}$), enabling sophisticated waveform generation and precise synchronization with external events or among multiple lasers.

3. METAL CUTTING

3.1 Background

Metal cutting is the largest industrial market for high-power lasers, with 2021 laser revenue estimated to be $> \$2$ billion.¹ This application was pioneered by CO₂ lasers. Fiber lasers have largely displaced CO₂ lasers because of their performance and practical advantages. In particular, for cutting of thin sheet with N₂ assist gas, fiber lasers offer significantly higher cutting speeds. CO₂ lasers maintained an advantage, however, for one important application: cutting of mild-steel plate (thickness above ~ 6 mm) with O₂ assist gas. In this application, CO₂ lasers offer significantly better edge quality than legacy, fixed-beam fiber lasers. As a result, job shops would have to either accept poor performance for mild-steel cutting or maintain both CO₂- and fiber-laser tools. The initial CFX products aimed to address this longstanding problem. Recent CFX designs, discussed below, have simultaneously enabled the N₂ cutting speed to be increased.

3.2 Initial CFX products

CFX fiber lasers were first offered at 3 – 5 kW with a three-zone design (100/215/330) and subsequently at 6 – 15 kW with a two-zone design (100/330). Figure 1 shows near-field spatial profiles and measured beam diameters for these lasers. Both products provide $\sim 3.5\times$ range in the D4 σ beam diameter, corresponding to $> 10\times$ dynamic range in the beam area directly from the feeding fiber.

For conventional (fixed-beam) fiber lasers at the 3 – 15 kW level, a 100 μm feeding fiber is the most common, and the 100 μm central core of CFX allows these lasers to replicate the performance of standard fiber lasers (i.e., high N₂ cutting speed for thin sheet). The larger and ring-shaped CFX beams, not available in legacy fiber lasers, provide a dramatic improvement in O₂ cutting performance for mild steel,^{4,9} achieving cutting speed and edge quality that equal CO₂ lasers. For example, Fig. 4 shows 20 mm mild steel samples from HK Laser & Systems, a global manufacturer of machine tools, comparing the performance of 4 kW CFX and CO₂ lasers. The parts are visually similar, and the measured edge roughness, perpendicularity, and cutting speed are identical. CFX thus provides CO₂-like performance for O₂ cutting of mild steel plate while maintaining the practical and cost advantages of fiber lasers³ (high efficiency, fiber beam delivery, no routine maintenance, high reliability, etc.). Furthermore, HK showed that the focus position process window was twice as large for CFX vs. standard fiber lasers (± 2 mm vs. ± 1 mm).

CFX has thus eliminated the one remaining advantage of CO₂ lasers over legacy fiber lasers in the important application of metal cutting. In addition:

- As expected, CFX Index 0 provides cutting speed and edge quality similar to conventional fiber lasers with 100 μm feeding fibers. This setting is typically employed with thin sheet to maximize the N₂ cutting speed.
- The aluminum edge quality obtained with CFX can be better than that obtainable with conventional fiber lasers at higher power, demonstrating the benefit of optimized delivery of laser power to the workpiece. This result was reported by the tool integrator Cincinnati.
- For N₂ cutting of stainless steel, Index > 0 can provide better edge quality than conventional (100 μm) fiber lasers with only a small speed penalty. The versatility of Corona-enabled cutting tools thus allows application-specific optimization the part specifications and cost. This result was reported by the tool integrator CYLASER.

These benefits are further discussed in Refs. 4 and 9.

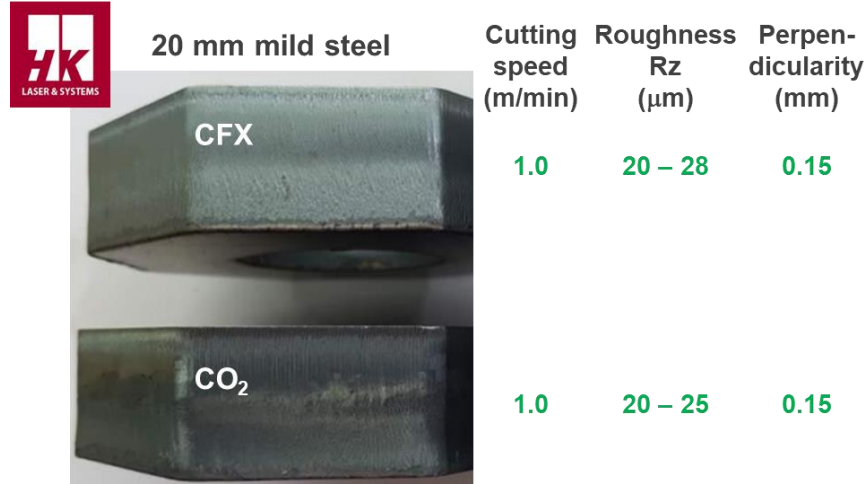


Figure 4. Comparison of O₂ cutting of 20 mm mild steel with a 4 kW CFX fiber laser (top) and a 4 kW CO₂ laser (bottom) performed by HK Laser & Systems. Photographs show the edges of the cut parts, and the corresponding cutting speed and measured edge roughness and perpendicularity are given to the right of the photographs.

CFX fiber lasers have enabled highly versatile or “universal” metal-cutting tools, and leading tool integrators have released CFX-based tools worldwide. End-users can now have a single tool that performs optimum cutting for a range of materials and thicknesses rather than tolerating poor performance for some jobs or supporting multiple tools.

3.3 New CFX products

Having addressed the problem of thick mild steel cutting with the large ring-shaped CFX beams, we next considered fiber designs to optimize N₂ cutting performance for thin sheet metal (another large application). It is known that smaller beams provide faster N₂ cutting speeds, and some tools employ a 50 μm rather than a 100 μm feeding fiber, although the maximum thickness is then further restricted. We redesigned the CFX feeding fiber to provide a 50 μm Index 0 beam for faster N₂ cutting while maintaining the 330 μm annular guiding region for O₂ cutting of mild steel (50/175/330 design). Figure 5 compares near-field spatial profiles for this product (known as Mach Ultra™) to those for the 100/215/330 design. The original CFX design provides a >10x dynamic range in beam area, and Mach Ultra increases the dynamic range to nearly 50x.

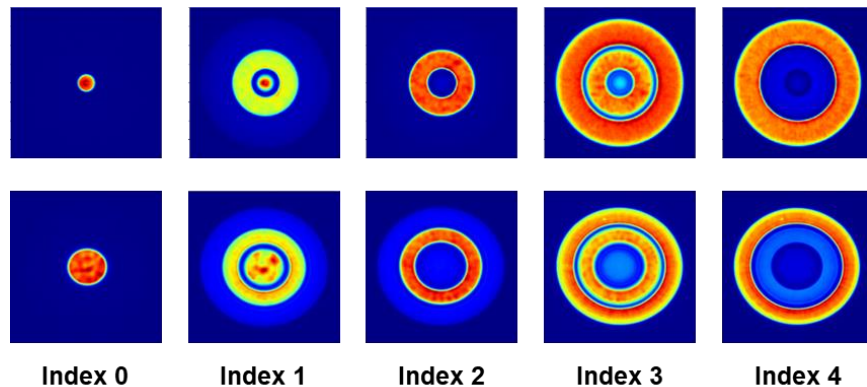


Figure 5. Near-field spatial profiles for three-zone CFX (3 – 5 kW) with a 100/215/330 design (bottom row) and the Mach Ultra 50/175/330 design (top row). The Mach Ultra design has reduced the od of the smallest beam (Index 0) by a factor of two (4x higher irradiance), while maintaining the 330 μm od of the largest beam (Index 4).

We validated the cutting performance of Mach Ultra for both N₂ and O₂ cutting. Figure 6 shows the N₂ cutting speed for 3 mm stainless steel for a conventional fiber laser (100 μm feeding fiber) at powers of 4 – 8 kW (grey bars). As expected, the cutting speed increases with laser power. The green bar in Fig. 6 shows the cutting speed for 5 kW Mach Ultra (Index 0). The Mach Ultra cutting speed at 5 kW is equivalent to that of a conventional fiber laser at 8 kW, dramatically illustrating the benefits of delivering the laser power in a more optimized format. The photograph in Fig. 6 shows the Mach Ultra cutting samples, and they have the excellent edge quality expected. The ability to use a lower laser power while maintaining the same cutting speed and edge quality provides a lower cost per manufactured part by reducing both the up-front cost (laser and chiller) and the operating costs (electricity, downtime for cleaning or replacing optics in the cutting head). Furthermore, Mach Ultra maintains excellent performance for O₂ cutting of mild steel using Index 4, as expected (Fig. 7).

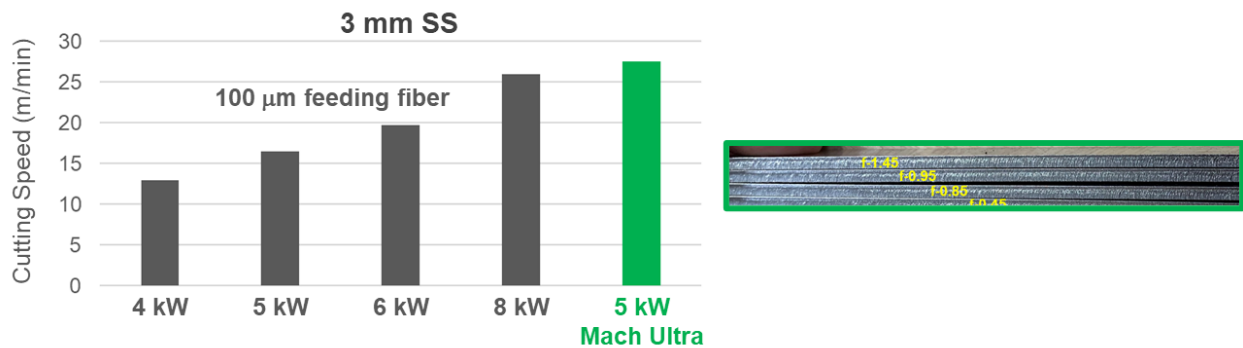


Figure 6. Cutting speed for 3 mm stainless steel with N₂ assist gas for a conventional fiber laser (100 μm feeding fiber) at 4, 5, 6, and 8 kW (grey bars) and for Mach Ultra (Index 0, 50 μm beam diameter) at 5 kW. All samples were cut using the same material on the same cutting tool with the same cutting head (2x magnification). The photograph on the right shows examples of the material cut with Mach Ultra.



Figure 7. Photographs of 19 mm mild steel cut using Mach Ultra (Index 4) with O₂ assist gas. The edge quality is excellent, as with other CFX fiber lasers.

With the Mach Ultra design, CFX is now able to simultaneously provide all the following benefits:

1. CO₂-like performance (excellent edge quality) for O₂ cutting of mild steel.
2. N₂ cutting speeds that are faster than conventional (100 μm) fiber lasers at the same power level and equal to those of tools optimized for thin metal only (50 μm feeding fiber). Stated differently, Mach Ultra provides the same N₂ cutting speed as conventional fiber lasers operating at significantly higher power levels.
3. The ability to optimize the edge quality vs. speed for N₂ cutting of stainless steel and aluminum.

The Corona fiber laser is the only technology that achieves the combination of performance and practical advantages described above, meeting all the goals listed in Section 2.2.

4. METAL WELDING

4.1 Background

Metal welding is the second-largest industrial market for high-power lasers¹, with significant growth driven by automotive applications. Lasers provide substantially higher throughput than conventional welding processes and can generate precise, low-heat-input welds, resulting in increased productivity and part quality. The high power and beam quality (high irradiance) of fiber lasers enables “keyhole welding,” characterized by a high-aspect-ratio penetration profile, fast travel speed, and minimal distortion or heat-affected zone. Use of a larger spot size (lower irradiance) results in a shallower “conduction weld,” which is advantageous for aesthetic reasons and for minimizing post-processing steps. Transitioning between these two welding modes and optimizing the welding performance for different materials and joint designs requires different beam properties at the workpiece.

4.2 CFX welding

Welding typically requires a larger number of Index settings than cutting to optimally tailor the weld profile. Figure 8 shows the near-field spatial profiles and calculated beam diameters for a two-zone (100/330) CFX fiber laser employed for welding. Note that the same laser design is also used for cutting, and the Index settings have simply been changed in the control software to facilitate welding process optimization (compare Fig. 8 with the right panel of Fig. 1).

The ability to tailor the weld profile using CFX can reduce the deleterious effects of spatter, porosity, and cracking, increase the process window, and/or provide a gap-bridging capability. Reference 10 presents analysis of CFX bead-on-plate welds, illustrating the transition from keyhole to conduction weld profiles. It also shows a demonstration of the ability of CFX to significantly reduce spatter in welding of a steel powertrain component by stabilizing the keyhole (i.e., by preventing episodic closure and reopening of the keyhole during the welding process). The reader is referred to Ref. 10 for more details.

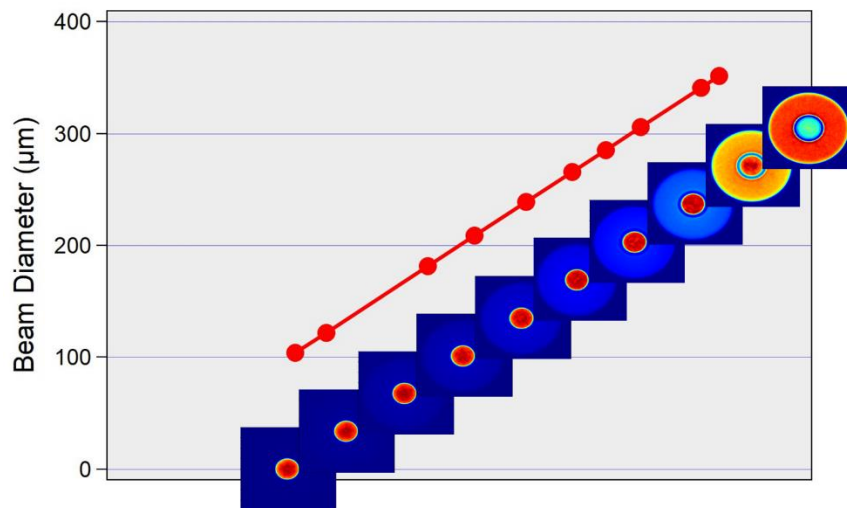


Figure 8. Typical beam settings for a two-zone (100/330) CFX fiber laser used in metal welding. The images show near-field spatial profiles, and the corresponding second-moment beam diameters are given on the y-axis. Note that the laser design is the same as that shown in Fig. 1 (right) with additional Index settings added for welding.

5. METAL ADDITIVE MANUFACTURING

5.1 Background

Additive manufacturing (AM) promises previously unimaginable production capabilities in both existing and emerging applications. Laser powder bed fusion (L-PBF) is the leading AM technology for producing high-quality, precision parts

from a wide range of metals and alloys. L-PBF productivity is limited, however, by long build times, restricting its use to high-cost parts or prototyping and preventing its deployment for series (high-volume) production. This productivity limitation stems from the use of single-mode (SM) lasers in L-PBF tools.

Typical parts include both fine detail and large-scale features. L-PBF tools employ SM lasers to enable production of fine features, but the resultant small spot size and Gaussian beam shape preclude faster production of larger features. Expanding the beam using a zoom lens does not address this problem because the resultant beam profile is still Gaussian, whose peaky shape causes overheating, resulting in generation of smoke, spatter, and porosity. Similarly, expanding the beam by working off-focus retains the nonoptimal Gaussian spatial profile, and this approach also reduces the process window because of the rapid change in beam size with position along the propagation direction. Instead, a beam shape that generates a flatter transverse temperature profile in the workpiece is needed. The optimum beam shape depends on multiple parameters, including the thermal properties of the powder and underlying material, the spot size, the scan speed, and the optical power. The ideal L-PBF laser source would thus provide a SM beam for producing fine features and a family of larger beams with optimized shapes for producing larger features. Initial analysis indicated that beams with ring and saddle shapes could generate the desired thermal profile. Until AFX, no laser source could provide this versatility.

5.2 AFX optical performance

The AFX feeding fiber has a 14/40 design, with the central core providing a SM beam, and the annular core providing a 40 μm od ring beam. Figure 9 shows AFX near-field spatial profiles, $D4\sigma$ beam diameters, and M^2 values for different Index settings (i.e., divisions of power between the central core and the ring). As noted for CFX, the standard beam parameters of diameter and M^2 do not provide a complete description of the AFX beams; we find the fractional division of the power between the two guiding regions to be a more relevant metric for heat deposition into the workpiece.

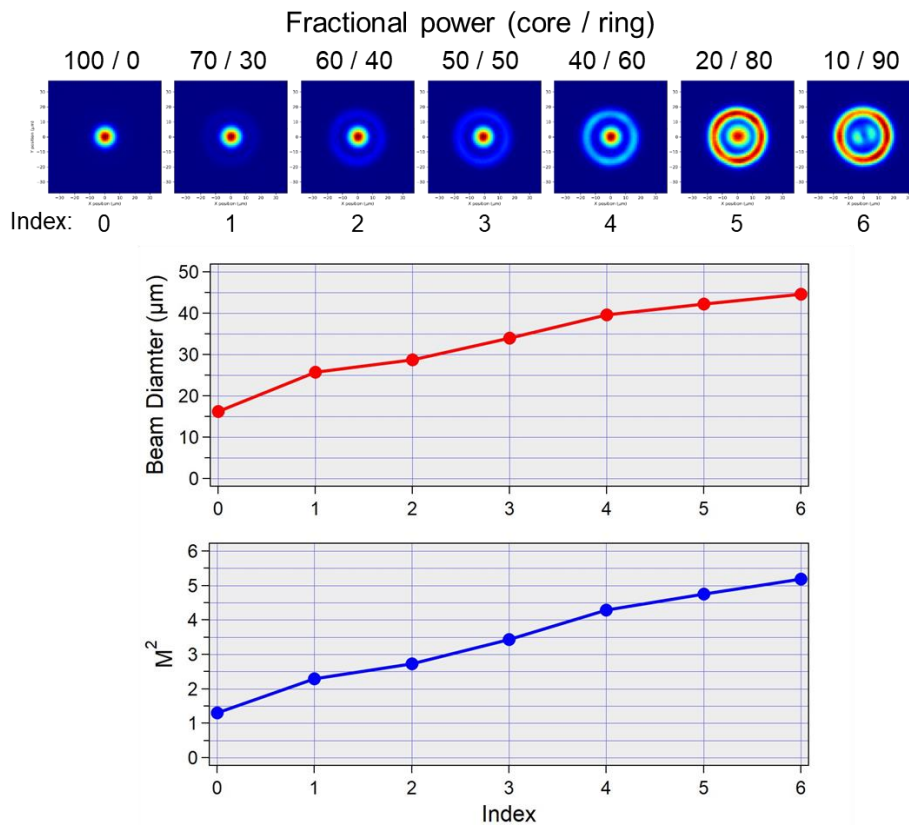


Figure 9. AFX Index settings. The top images show near-field spatial profiles for the indicated divisions of power between the central core and the ring. The upper graph shows the calculated $D4\sigma$ beam diameters, and the lower graph shows the corresponding M^2 values.

The AFX SM beam (Index 0) has a slightly different beam shape than a conventional SM fiber laser because of a small amount of power in the ring, resulting in a calculated $D4\sigma M^2$ value that is ~10% higher. Optical measurements verify that the AFX Index 0 beam has the same propagation characteristics as a conventional SM fiber laser beam. More importantly, L-PBF results from multiple groups using a number of materials show that AFX Index 0 provides performance identical to that of standard SM fiber lasers. AFX-equipped L-PBF tools are thus capable of producing the required fine-scale features using the Index 0 setting.

An advantage of SM lasers is that they provide a large depth of focus (Rayleigh range, Z_R), resulting in a large process window. The Rayleigh range is given by $Z_R = \pi \omega_0^2 / (M^2 \lambda)$, where ω_0 is the radius at the beam waist and λ is the wavelength. Although the AFX beams with Index > 0 are multimode ($M^2 > 1$), they retain excellent beam quality and thus a large depth of focus. Figure 10 shows Z_R values for each Index setting for magnification values between 4 and 6 (typical for L-PBF tools). Note that Z_R increases with increasing Index despite the higher M^2 value (because the effect of the larger ω_0 is dominant). AFX fiber lasers thus provide larger beams with optimized shapes for L-PBF while retaining a large process window for all Index settings.

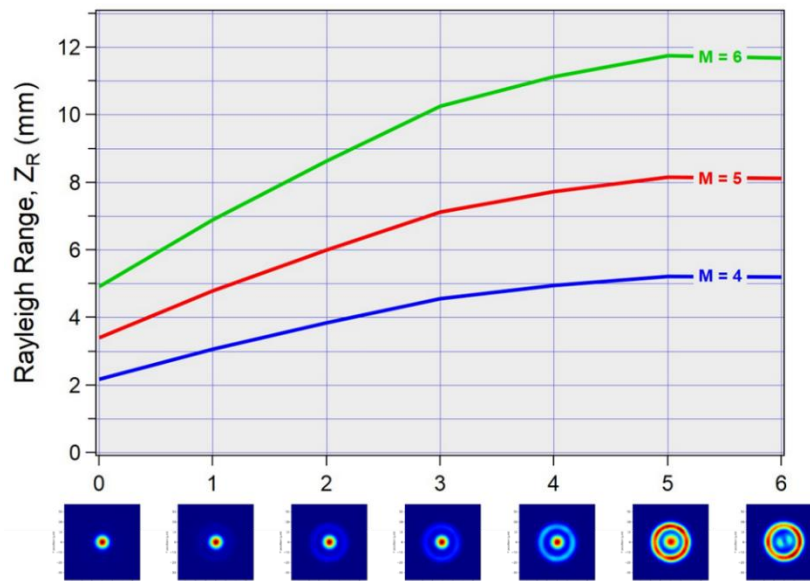


Figure 10. Z_R vs. AFX Index setting for magnifications of 4 (blue), 5 (red), and 6 (green). Note that Z_R increases with Index even though the beams with Index > 0 are multimode ($M^2 > 1$, see Fig. 9).

Some methods for generating ring beams and other shapes provide the desired shape only near the beam waist, resulting in a small process window. In contrast, AFX beams retain the desired shape over a significant distance because of their excellent beam quality. For example, Fig. 11 shows spatial profiles and the beam caustic (diameter vs. position along the propagation direction, z) for the AFX beam with the largest M^2 value (Index 6) for a magnification of 5.2. As seen in the beam profiles, the beam maintains a ring shape over nearly ± 4 mm (or $\pm 1/2 Z_R$); similar results are observed for other magnifications and Index settings. Thus, for typical magnifications, AFX beam profiles retain the desired shape over $\pm 3 - 4$ mm, resulting in a large process window.

AFX is available at power levels up to 1.2 kW. To avoid stimulated Raman scattering, when supplied with a 5 m feeding fiber, the Index 0 – 2 power is limited to 850 W, and the Index 3 power is limited to 1050 W (of course, higher powers are available with shorter feeding fibers). Full power is available in Index 4 – 6.

Finally, nLIGHT has developed a family of collimators to facilitate AFX tool integration. These collimators feature diffraction-limited optics that maintain beam quality over the full power range for all Index settings. They are designed for high optical power and brightness, with near-zero focus shift and no thermally induced aberrations. They are available with seven focal lengths between 50 and 160 mm. These collimators include an optional 0.10 NA aperture to ensure no beam clipping on scanner input apertures or process optics. The collimator maintains all beam specifications when being added or changed in the field (i.e., a given collimator is not paired with a given laser).

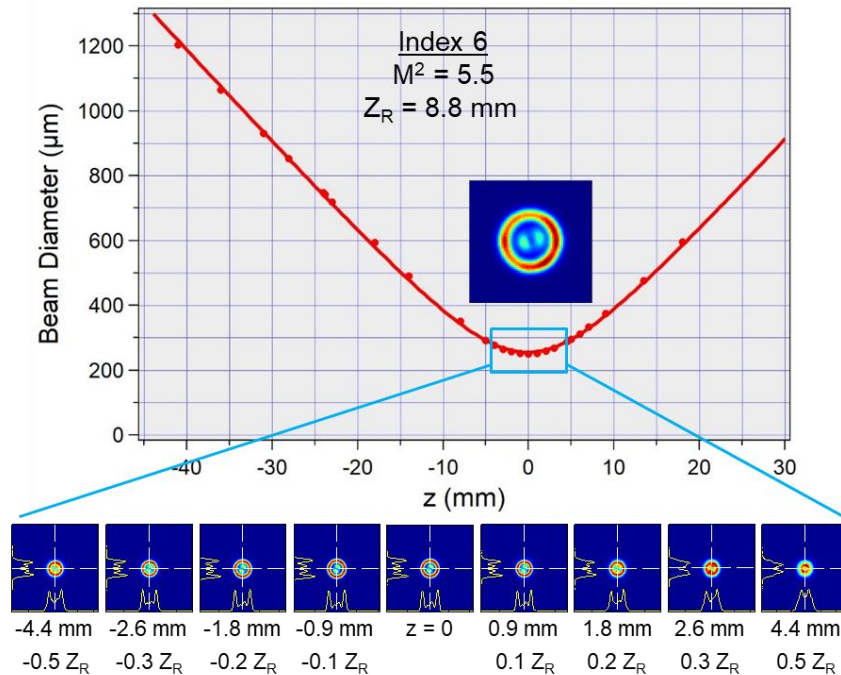


Figure 11. Beam diameter vs. z (position along the propagation direction) for AFX Index 6. The magnification was 5.2 (a typical value for L-PBF tools). The lower images show the beam profiles at the indicated positions near the beam waist.

5.3 AFX L-PBF results

Several L-PBF tool integrators and research laboratories have demonstrated and quantified the benefits of AFX for L-PBF productivity and part quality, and recent results were presented at Formnext (the largest AM tradeshow) in November 2021.¹¹⁻¹⁵

For example, Aconity3D showed that AFX can increase the build rate for titanium by 7.8x, from 5.4 cm³/hr for a standard SM fiber laser to 42.1 cm³/hr for AFX. Such a large increase in productivity is groundbreaking, completely changing the economics of L-PBF manufactured parts. This dramatic result was achieved because AFX enabled simultaneous increases of both the scanning speed and the melted volume while maintaining excellent material quality (>99.8% density). In other work, Aconity3D showed that AFX can control the microstructure and thus the material properties of Inconel 718. This capability is relatively unexplored and offers significant possibilities for production of unique components and features using L-PBF.

A group at the Technical University of Munich (TUM) showed that AFX can simultaneously increase the build rate (by ~2x) and the process window for L-PBF of stainless steel.¹⁶ Figure 12 shows the power and scanning speed when using a SM Gaussian beam and when using AFX Index 5. This figure shows that AFX enabled use of higher power and thus a faster scanning speed (higher productivity) with a larger process window (i.e., good part quality over a range of powers).

Figure 13 summarizes the TUM findings and shows examples of part cross sections used to establish the process window. This figure shows that the power of the Gaussian beam cannot be increased without an undesirable balling effect, which limits the productivity of L-PBF tools equipped with SM lasers. In contrast, the AFX power for Index settings of 4 – 6 can be increased without balling, providing a higher build rate with excellent part quality.

AFX was released in November 2020 and has thus been on the market for a relatively short time. Nonetheless, it is already paving the way for a new generation of high-productivity L-PBF tools for series production.

REFERENCES

- [1] D.A. Belforte, *Laser Focus World*, Vol. 57, No. 2, p. 17 (February 2021).
- [2] B. Victor and D. Kliner, *Shop Floor Lasers*, p. 11 (March/April 2018).
- [3] D.A.V. Kliner and L. Sheehan, *Photonics & Imaging Technology*, p. 2 (March 2017).
- [4] B. O'Dea *et al.*, in *Laser Beam Shaping XIX*, edited by A. Dudley and A.V. Laskin, Proc. of SPIE Vol. 11107, 111070J (2019).
- [5] D.A.V. Kliner, R.L. Farrow, and B. Victor, *Laser Focus World*, Vol. 55, No. 4, p. 45 (April 2019).
- [6] D.A.V. Kliner and R.L. Farrow, US Patent No. 10,295,845 (issued May 21, 2019).
- [7] D.A.V. Kliner *et al.*, in *Components and Packaging for Laser Systems IV*, edited by A.L. Glebov and P.O. Leisher, Proc. of SPIE Vol. 10513, 105130S (2018).
- [8] D.A.V. Kliner, J. Bell, and L. Sheehan, *Industrial Laser Solutions*, Vol. 31, Issue 2 (March, 2016)
- [9] D. Kliner and B. Victor, *Industrial Laser Solutions*, Vol. 33, Issue 5, p. 23 (September/October 2018).
- [10] B. Victor, D. Kliner, and M. Hepp, *Industrial Laser Solutions*, Vol. 34, Issue 5, p. 9 (September/October 2019).
- [11] www.youtube.com/watch?v=OVemoWOtu5w
- [12] www.youtube.com/watch?v=OjUj23tH4fg
- [13] www.youtube.com/watch?v=wbMEf1i28Ko&list=PLeXialZMPNVqcwiLdFAecX8I1xvodCIuK&index=5
- [14] www.youtube.com/watch?v=bvqBRtGxwCY&list=PLeXialZMPNVqcwiLdFAecX8I1xvodCIuK&index=6
- [15] www.youtube.com/watch?v=2kuBftrrbK4
- [16] J. Grünewald, F. Gehringer, M. Schmöllner, and K. Wudy, *Metals* 11, 1989 (2021).